

RESEARCH

Open Access



Genetic variation reveals the therapeutic potential of *BRSK2* in idiopathic pulmonary fibrosis

Zhe Chen^{1†}, Mingyang Tang^{2†}, Nan Wang^{1†}, Jiangjiang Liu¹, Xiaoyan Tan¹, Haitao Ma^{1*}, Jing Luo^{3*} and Kai Xie^{1*}

Abstract

Background Current research underscores the need to better understand the pathogenic mechanisms and treatment strategies for idiopathic pulmonary fibrosis (IPF). This study aimed to identify key targets involved in the progression of IPF.

Methods We employed Mendelian randomization (MR) with three genome-wide association studies and four quantitative trait loci datasets to identify key driver genes for IPF. Prioritized targets were evaluated for respiratory insufficiency and transplant-free survival. The therapeutic efficacy of the core gene was validated in cellular and animal models. Additionally, we conducted a comprehensive evaluation of therapeutic value, pathogenic mechanisms, and safety through phenome-wide association study (PheWAS), mediation analysis, transcriptomic analyses, shared causal variant exploration, DNA methylation MR, and protein interactions.

Results Multiple MR results revealed that *BRSK2* has a significant pathogenic impact on IPF at both transcriptional and translational levels, with a lung tissue-specific association (OR = 1.596; CI, 1.300–1.961; $P_{val} = 8.290 \times 10^{-6}$). *BRSK2* was associated with IPF progression driven by high-risk factors, with mediation effects ranging from 34.452 to 69.665%. Elevated *BRSK2* expression in peripheral blood mononuclear cells correlated with reduced pulmonary function, while increased circulating *BRSK2* levels suggested respiratory failure and shorter transplant-free survival in IPF patients. *BRSK2* silencing attenuated lung fibrosis progression in cellular and animal models. Transcriptomic integration identified *PSMB1*, *CTSD*, and *CTSH* as significant downstream effectors of *BRSK2*, with *PSMB1* showing robust shared causal variant support (PPH4 = 0.800). Colocalization analysis and phenotype scan deepened the pathogenic association of *BRSK2* with IPF, while methylation MR analysis highlighted the critical role of epigenetic regulation in *BRSK2*-driven IPF pathogenesis. PheWAS revealed no significant drug-related toxicities for *BRSK2*, and its therapeutic potential was further underscored by protein interaction analyses.

Conclusions *BRSK2* is identified as a critical pathogenic factor in IPF, with strong potential as a therapeutic target. Future studies should focus on its translational implications and the development of targeted therapies to improve patient outcomes.

Keywords Causal pathways, Idiopathic pulmonary fibrosis, Therapeutic targets, *BRSK2*

[†]Zhe Chen, Mingyang Tang, and Nan Wang are joint first authors.

*Correspondence:

Haitao Ma

mhtszdx@163.com

Jing Luo

luojing_2767983@163.com

Kai Xie

kaixie715786420@126.com

Full list of author information is available at the end of the article



Background

Idiopathic pulmonary fibrosis (IPF) is a chronic, progressively worsening disease of the lung interstitium, characterized by a marked decline in lung function and an invariably poor prognosis [1]. Despite increasing prevalence, the treatment options for IPF remain severely limited. Current pharmacological therapies, such as pirfenidone and nintedanib, offer only modest benefits in terms of disease progression and survival, and many patients suffer from significant adverse effects [2], highlighting an urgent need for more effective and tolerable treatments.

Recent large-scale genetic research has highlighted several potential drug targets, such as kinesin family member 1 (*KIF15*), mitotic arrest deficient 1 like 1 (*MAD1L1*), DEP domain-containing MTOR interacting protein (*DEPTOR*), and mucin 5B (*MUC5B*) [3, 4]. Despite these breakthroughs, the complex etiology of IPF complicates the transition of these discoveries into practical treatments, impeding the development of innovative therapies and limiting our understanding of IPF's fundamental biological mechanisms. This highlights an urgent need for specialized research approaches that can dissect the intricate biological processes of IPF. Employing these advanced methodologies will be crucial in identifying and validating more effective treatment targets, thereby accelerating the path from genetic insight to clinical application.

Mendelian randomization (MR) serves as a robust method for discerning causal relationships between genetic variants and disease outcomes, utilizing these variants as instrumental variables (IVs). This approach minimizes the confounding influences commonly encountered in observational studies [5], offering a distinctive opportunity to clarify the causal pathways implicated in IPF and to identify innovative therapeutic targets anchored in genetic evidence.

In our study, we employed an exhaustive MR methodology, utilizing genetic proxies derived from expression quantitative trait loci (eQTLs), protein quantitative trait loci (pQTLs), and genome-wide association studies (GWAS) to identify and prioritize therapeutic targets for IPF. Subsequent validation of the core target was conducted through cellular and animal models. Additionally, our research included genetic correlation analyses, drug safety assessments, mediation analyses, phenotypic scanning, transcriptomic analyses, analyses of methylation and epigenetic regulation, and protein interaction evaluations. These comprehensive analyses underscore the substantial translational potential and biological significance of the prioritized target, suggesting its clinical applicability in personalized therapeutic strategies for IPF.

Methods

Study design

Our study design, illustrated in Fig. 1, employs a comprehensive approach using multiple data sources and detailed analytical methods to identify the core causative molecules of IPF and explore their pathogenic potential and underlying mechanisms.

Data sources

Detailed information regarding the data sources is provided in Additional file 1: Table S1. Briefly, we incorporated QTL data from five sources and outcome GWAS data from three sources [6–13]. The GWAS data for potential risk factors (PRFs) were obtained from several large-scale studies [14–16].

Mendelian randomization analysis

TSMR analysis was performed using the TwoSampleMR R package with default parameters. Separate datasets were used for exposures and outcomes to avoid significant sample overlap. The instrumental variables (IVs) were selected based on the following criteria: (1) QTL data confirmed as protein-coding by the Ensembl website; (2) IVs with a minor allele frequency (MAF) > 0.01; (3) correlation *P*val of IVs with traits < 5e-8; (4) IVs located outside the major histocompatibility complex [17]; (5) IVs pruned through linkage disequilibrium ($r^2 > 0.001$, kb = 1000); (6) IVs with an *F* statistic > 10 [18]; (7) Cis-variant loci (IVs within 1MB upstream or downstream of the gene) used as Cis-QTLs. IVs for IPF and PRFs strictly adhered to criteria (2), (3), (5), and (6). Heterogeneity and horizontal pleiotropy were assessed using Cochran's *Q* test and the MR Egger intercept method (*P*val < 0.05 indicating statistical significance). The constrained maximum likelihood and model averaging (cML-MA) method was used to control for correlated and uncorrelated horizontal pleiotropy [19]. Goodness-of-fit (GOF) tests used the BIC (Bayesian information criterion) method for *P*vals < 0.05, and the BIC-DP (data perturbation) method otherwise. Directionality tests were conducted to assess reverse causality, with the result "TRUE" indicating that no statistical reverse causality was present in the TSMR results. To evaluate the overall effects of TSMR analyses at transcriptional and translational levels, we assessed heterogeneity using the *I*² statistic, with values > 50% indicating statistically significant heterogeneity, and applied a random-effects meta-analysis to integrate effect estimates.

Our main findings were validated using summary data-based Mendelian randomization (SMR) analysis [20]. Additionally, we examined the relationship between *BRSK2* transcriptional and translational levels and

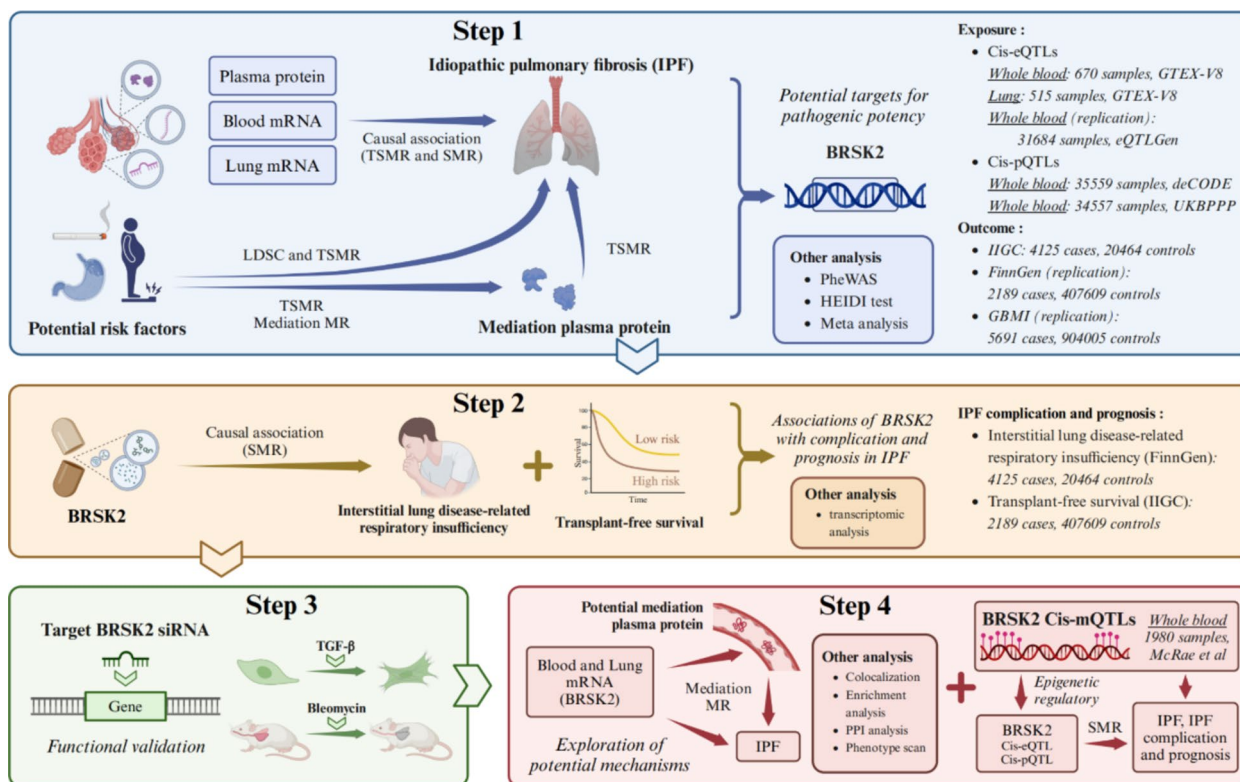


Fig. 1 Overall study design and analysis flowchart. Comprehensive TSMR analysis was performed using eQTL, pQTL, and GWAS data from multiple sources, followed by the application of the HEDI test to identify *BRISK2* as a core therapeutic target for IPF. Causal and correlation analyses revealed the detrimental effects of *BRISK2* on respiratory function, IPF complications, and prognosis. Subsequently, in vitro and in vivo experiments were conducted to further elucidate the anti-pulmonary fibrosis potential of *BRISK2*. Additionally, we conducted a series of supplementary analyses, including meta-analysis, mediation analysis, colocalization analysis, transcriptomic analysis, DNA methylation analysis, protein association analysis, PheWAS analysis, and phenotype scanning, to further investigate the therapeutic mechanisms and clinical value of *BRISK2*. TSMR, two-sample Mendelian randomization; SMR, summary data-based Mendelian randomization analysis; HEIDI, heterogeneity in the dependent instrument; PheWAS, phenome-wide association study; GWAS, Genome-Wide Association Studies; eQTL, expression quantitative trait loci; pQTL, protein quantitative trait loci; mQTL, methylation quantitative trait loci; IPF, idiopathic pulmonary fibrosis; IIGC, International IPF Genetics Consortium; GBMI, Global Biobank Meta-analysis Initiative

respiratory insufficiency in interstitial lung disease (ILD) and transplant-free survival. We also assessed causal links between DNA methylation levels and both the onset and progression of the disease, in conjunction with *BRISK2* expression levels [21, 22]. A $P_{val} > 0.01$ for the heterogeneity in dependent instruments (HEIDI) test indicated that the gene expression causality was not driven by linkage disequilibrium in SNPs [23]. Our study strictly follows the previously published reporting guidelines for observational studies in epidemiology using Mendelian randomization [24].

Other analysis

In 470,000 participants of the UK Biobank cohort [25], a phenome-wide association study (PheWAS) was conducted to ensure the exclusivity of MR and to detect potential adverse effects of the target. We also performed

a phenotype scan using the IEU Open GWAS project web tool (<https://gwas.mrcieu.ac.uk/>) for IVs of the core target, and to avoid pleiotropy, these features should not include IPF confounders.

Posterior probabilities (PP) for five hypotheses were calculated using Bayesian colocalization analysis in the COLOC package. Positive outcomes of the colocalization analysis included $PPH4 > 0.5$ and $PPH3 + 4 > 0.8$, with $PPH4 > 0.8$ being strong evidence, indicating a high likelihood that the exposure and outcome are influenced by shared genetic variants in the same region [26, 27]. Furthermore, the strong association ($P_{val} < 5 \times 10^{-8}$) between IV and IPF-related characteristics in the results of the phenotype scan also suggests potential evidence of shared causal variation.

Normalized, log-transformed transcriptomic data from the GSE213001 [28] and GSE38958 [29] datasets

were analyzed to assess *BRSK2* expression in lung tissue and peripheral blood mononuclear cells (PBMCs) from idiopathic pulmonary fibrosis (IPF) patients and healthy controls. The GSE38958 dataset also included quantitative phenotypic measures such as DLCO and FVC%pred, enabling detailed analysis. Spearman correlation was used to examine the association between *BRSK2* expression and pulmonary function metrics, with statistical significance set at $Pval < 0.05$. Additionally, *BRSK2* expression and its downstream targets were analyzed in IPF lung tissue data from Furusawa et al. [30], identifying significant targets with an absolute correlation coefficient > 0.4 .

Kyoto Encyclopedia of Genes and Genomes (KEGG) visualization was performed using the OmicShare tool (<https://www.omicshare.com/tools/>).

Although the actions of targeted drugs in clinical trials are well-documented, interactions between core molecules and therapeutic targets in IPF remain unclear. To investigate, we retrieved IPF drug target data from clinical trials (<https://clinicaltrials.gov>) and performed protein–protein interaction (PPI) analysis using GENEMANIA (<https://genemania.org>) to clarify links between *BRSK2*, known IPF targets, and additional targets identified in this study.

In vitro and in vivo experiments

Cell culture

MLE-12 and A549 cells from the Shanghai Cell Bank of the Chinese Academy of Sciences were cultured in DMEM with 10% fetal bovine serum and 1% penicillin/streptomycin. Cells were maintained at 37 °C in a humidified atmosphere with 5% CO₂.

Animal model construction

Male C57BL/6 mice were divided into three groups ($N=4$ per group): PBS group, control group (PEI/siCtrl), and treatment group (PEI/si-*BRSK2*). PEI/siCtrl and PEI/si-*BRSK2* group were anesthetized with 1% pentobarbital sodium (60 mg/kg) and given 50 μL of intratracheal bleomycin (MERCK, #HY-17565A) in PBS [31]. After 7 days, Polyethylenimine/small interfering RNA (PEI/siRNA) complexes were prepared using low molecular weight branched PEI in HN buffer [32] per established methods [33]. The study was approved by the Institutional Animal Care and Use Committee at Soochow University Medical Center (the Fourth Affiliated Hospital of Soochow University, Suzhou Dushu Lake Hospital) Laboratory Animal Center (Application ID:241,136). The work has been reported in line with the ARRIVE criteria [34].

ELISA analysis

ELISA plates were coated with capture antibodies and incubated overnight at 4 °C. After blocking and washing, 100 μL of homogenized sample was added to each well, followed by a diluted detection antibody. Streptavidin-HRP was then added and incubated for 20 min at room temperature. Absorbance was measured at 450 nm using a spectrophotometer.

Analysis of lung tissue homogenate

Lung tissue was homogenized in 1 mL PBS and centrifuged at 2000 rpm for 10 min. The supernatant was collected, and inflammatory cytokine concentrations were measured using Mouse IL-1β and TNFα ELISA Kits according to the manufacturer's instructions.

Hydroxyproline assay

Lung tissue was hydrolyzed in 1 mL of solution in a boiling water bath for 20 min. The pH was adjusted to 6.0–6.8, followed by the addition of 10 mL distilled water and thorough mixing. Activated charcoal was then added to the diluted hydrolysate. After centrifugation, the clear supernatant was collected for further analysis. The hydroxyproline concentration in the lung tissue was measured using a specific kit following the provided instructions.

Statistical analysis

The GenomicSEM R package uses a built-in linkage disequilibrium score regression (LDSC) algorithm to calculate genetic correlations between traits ($Pval < 0.05$ indicates significance) and assess sample overlap between PRFs and IPF via the genetic covariance intercept. An intercept value close to zero suggests negligible sample overlap between the phenotypes.

Harmonized data for single and multiple IVs were analyzed using the wald ratio and inverse variance weighted (IVW) methods. Drug targets that remain statistically significant after Bonferroni correction were considered positive drug targets. Statistically significant results were defined as $Pval < 0.05$ after Bonferroni correction, while suggestive findings had $Pval$ between the significance threshold and 0.05. The number of each correction is equal to the product of the number of species of exposure and the number of species of outcome in a single analysis. Odds ratios (OR) for increased risk of IPF were expressed as per standard deviation (SD) increase in mRNA or plasma protein levels, and the presence of PRFs.

Since multi-factor MR analysis needs to integrate multiple exposed proxy variants, and there are very few cis-IVs of genes, the construction of a mediation network through multivariate MR analysis may lead to the loss

of IVs and result distortion. Therefore, we adopted two-step TSMR to estimate the mediation effect of plasma protein in the occurrence of IPF [35], and on the premise of reducing pleiotropy interference, MR analysis is less affected by confounding factors, so the mediation analysis combined with cML-MA analysis relatively reduces the potential impact of confounding bias. TSMR pathways with effect values (β) less than 0 and those with reverse causality were excluded. TSMR results with suggestive *Pval* were used to construct mediating pathways to detect more pathogenic effects. Confidence intervals and the significance of mediating effects were estimated using a bootstrap method with 1000 iterations. A *Pval* < 0.05 indicated a valid mediator.

All statistical analyses were performed using SPSS (version 22.0). Data visualization was done with GraphPad Prism (version 8.0) and R (version 4.3.3). Two-group comparisons used an unpaired, two-tailed Student's *t*-test. Data are expressed as mean \pm SD. A two-tailed *Pval* below 0.05 was considered statistically significant.

Results

Screening candidate druggable genes for IPF

The screening methodology for identifying potential IPF drug targets is illustrated in Additional file 2: Fig. S1, and relevant IV information for the TSMR analyses is detailed in Additional file 3: Supplementary Material. Our analysis encompassed 4615 Cis-eQTLs and 2716 Cis-pQTLs (Additional file 1: Tables S2–S7). The IVW or Wald ratio analysis identified 17 IPF drug targets, including *DECR2*, *MRM2*, *POLR2L*, *STN1*, *ZFYVE19*, *ARL17A*, *BRSK2*, *DEPTOR*, *DSCC1*, *KANSL1*, *LRRC37A*, *LRRC37A2*, *MAPT*, *PIDDI*, *WNT3*, *MUC2*, and *USP28* (Fig. 2A–D). In a joint replication analysis combining multiple exposures and outcomes, these targets were further validated using 15 MR combinations and additional methods such as cML-MA and SMR. At a significant level with a *Pval* threshold of 0.05/34 (1.471×10^{-3}), *BRSK2* emerged with the highest number of positive causal associations (Additional file 2: Figs. S2–S4), with its elevated expression levels strongly linked to increased IPF risk at both the transcriptional and translational levels, *LRRC17A2* has also been implicated in IPF-protective effects at the mRNA and translational levels, and the remaining targets have been verified to varying degrees in different MR combinations. Subsequent analyses showed no evidence of heterogeneity, pleiotropy, or reverse causality (Additional file 1: Tables S8–S12). Significantly, SMR results indicated that *BRSK2* expression in lung tissue and data from two IPF sources passed the HEIDI test (Fig. 2E, Additional file 1: Table S13), suggesting that *BRSK2* expression in lung tissue and the occurrence of IPF may be driven by shared causal variants, and the occurrence

of *BRSK2* and IPF may be more worthy of attention. Furthermore, a meta-analysis of TSMR results integrating transcriptional and translational levels consistently demonstrated a significant pathogenic effect of *BRSK2* (*Pval* significance threshold = 1.471×10^{-3}) (Additional file 2: Figs. S5–S6). Previous studies have associated risk factors such as smoking, gastro-esophageal reflux disease, and high BMI with elevated IPF risk [36–38], with both LDSC and TSMR analyses supporting these associations (Table 1, Additional file 1: Tables S14–S15). The low genetic covariance intercept from LDSC suggests a relatively minor bias in MR results due to sample overlap. To explore the potential pathogenic role of the core molecules in IPF high-risk populations, we further revealed the pathogenic potency of *BRSK2* in the population of PRFs by constructing a plasma protein network, and mediation analysis highlighted that plasma *BRSK2* protein plays a pathogenic role in mediating PRFs to IPF, with effect percentages ranging from 34.452 to 69.665% (Additional file 1: Tables S14–S15, Fig. 2F, Additional file 2: Fig. S7). In summary, MR analysis showed that *BRSK2* obtained a high level of evidence for the pathogenic effects of IPF at different levels.

PheWAS analysis

To address potential pleiotropic bias in MR and evaluate adverse drug reactions, we conducted a PheWAS using significant variations in *BRSK2* extracted by the same method as in MR analysis. The analysis included 5294 dichotomous and 6915 continuous variables across 14 phenotypic categories. No associations exceeded the significance threshold of *Pval* < 4.095×10^{-6} , with the most significant phenotype being the volume of gray matter in the right temporal pole (*Pval* = 1.405×10^{-5}) (Additional file 1: Tables S16–S17, Additional file 2: Fig. S8). PheWAS results suggested that the causal association of *BRSK2* and IPF receiving pleiotropic effects may be modest and that treatments targeting *BRSK2* are potentially safe.

BRSK2's role in IPF complications and prognosis

To further explain the association between *BRSK2* expression and complications and prognosis during the development of IPF as well as the possibility of shared variant driving, we evaluated the relationship between *BRSK2* expression and ILD-associated respiratory insufficiency and transplant-free survival in patients with IPF. Following Bonferroni correction (*Pval* < 0.05/4), SMR results indicated that elevated *BRSK2* protein levels (deCODE study, rs4881748 proxy) are associated with ILD-related respiratory insufficiency (OR = 3.879; CI, 2.058–7.311; *Pval* = 2.754×10^{-5}) and reduced transplant-free survival (OR = 0.481; CI, 0.240–0.964; *Pval* = 3.909×10^{-2}) in IPF patients. Additionally, *BRSK2*

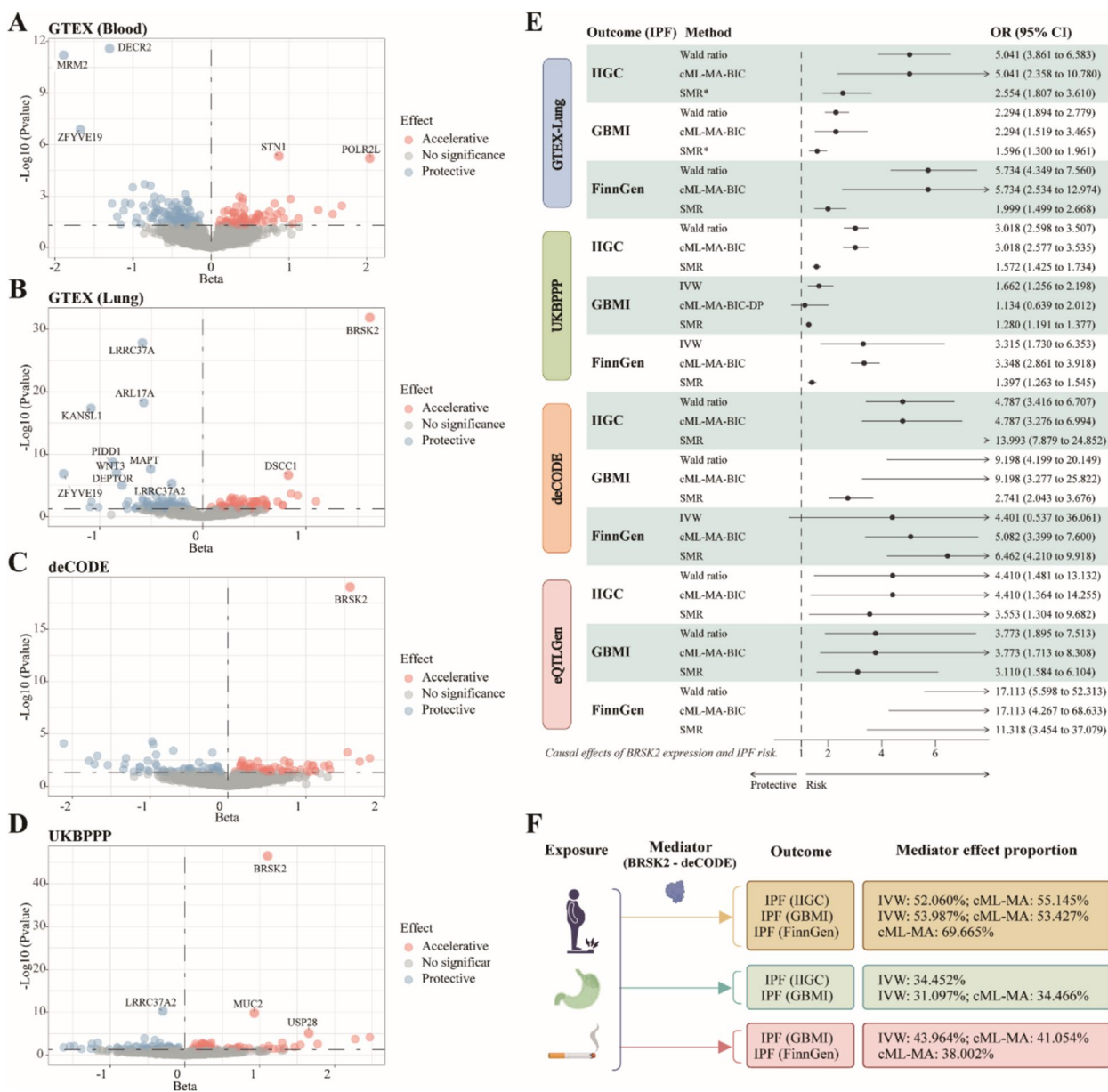


Fig. 2 Finding potential therapeutic targets for IPF. TSMR analyses were conducted to assess the association between blood mRNAs from GTEX (A), lung mRNAs from GTEX (B), plasma proteins from deCODE (C), plasma proteins from UKBPPP (D), and the risk of developing IPF. A beta value greater than 0 indicates that an increase in gene expression level promotes the occurrence of the disease. The gene names annotated in the figure represent IPF therapeutic targets that remain statistically significant ($Pval < 0.05$) after Bonferroni correction ($Pval < 0.05/4615$ for eQTLs TSMR and $Pval < 0.05/2716$ for pQTLs TSMR). **E** Forest plots of *BRISK2* and IPF risk by three MR methods. * means $Pval$ (HEIDI) > 0.01 . **F** Mediation effect of plasma protein *BRISK2* in promoting IPF in PRFs. TSMR, two-sample Mendelian randomization; IPF, idiopathic pulmonary fibrosis; IVW, inverse variance weighted; cML-MA, constrained maximum likelihood and model averaging; BIC, Bayesian information criterion; DP, data perturbation SMR, summary data-based Mendelian randomization; HEIDI, heterogeneity in the dependent instrument; OR, odds ratios; CI, confidence interval; IIGC, International IPF Genetics Consortium; GBMI, Global Biobank Meta-analysis Initiative

expression levels (eQTLGen-rs11603658) (OR=5.802; CI, 1.118–30.105; $Pval = 3.634 \times 10^{-2}$) and translation levels (UKBPPP-rs7395567) (OR=1.191; CI, 1.006–1.411; $Pval = 4.200 \times 10^{-2}$) were also linked to respiratory insufficiency in IPF patients at suggestive significance levels.

External validation using RNA-seq analysis revealed significantly higher *BRISK2* expression levels in lung lesions and PBMCs of IPF patients compared to controls. Moreover, *BRISK2* expression levels in PBMCs of IPF patients were significantly negatively correlated with DLCO and

Table 1 LDSC analysis results of PRFs and IPFs

Exposure	Outcome (IPF)	Correlation coefficient	Se	Pval	Genetic covariance intercept
Body mass index	GBMI	0.318	0.049	8.460E-11	-1.360E-02
Body mass index	FinnGen	0.132	0.058	2.222E-02	-8.000E-03
Body mass index	IIGC	0.123	0.030	5.033E-05	2.400E-03
Gastroesophageal reflux disease	GBMI	0.394	0.048	3.612E-16	1.200E-02
Gastroesophageal reflux disease	FinnGen	0.231	0.054	1.662E-05	-1.010E-02
Gastroesophageal reflux disease	IIGC	0.154	0.038	6.095E-05	3.000E-04
Smoking initiation	GBMI	0.266	0.051	2.339E-07	5.200E-03
Smoking initiation	FinnGen	0.180	0.053	7.502E-04	2.600E-03
Smoking initiation	IIGC	0.075	0.035	3.378E-02	-7.800E-03

LDSC linkage disequilibrium score regression, IIGC International IPF Genetics Consortium, GBMI Global Biobank Meta-analysis Initiative, PRFs potential risk factors, IPF idiopathic pulmonary fibrosis

FVC%pred values (Additional file 2: Fig. S9). These findings align with the main analyses and suggest a potentially harmful role for *BRSK2* in IPF progression (Table 2).

***BRSK2* deficiency alleviates bleomycin-induced pulmonary fibrosis in vitro and in vivo**

Our findings identified *BRSK2* as a potential driver in IPF progression. To explore its role further, we conducted experiments to confirm its function in IPF. We used the TGF-β1 signaling pathway, a key regulator in fibrogenesis, to induce fibroblast differentiation in MLE-12 cells with 10 ng/mL TGF-β1 (Fig. 3A). By day three, Masson’s trichrome staining confirmed successful differentiation, shown by notable morphological changes (Fig. 3B). *BRSK2*-siRNAs effectively reduced *BRSK2* expression in these TGF-β1-treated cells (Fig. 3C). Additionally, *BRSK2* inhibition decreased TGF-β1-induced cellular proliferation, as shown by CCK-8 and EdU fluorescence assays, and lowered α-SMA and Col1A1 expression (Fig. 3D, E). ELISA results showed increased IL-1β and IL-6 secretion following TGF-β1 treatment, but siRNA treatment reduced these cytokine levels, indicating that *BRSK2*

modulates TGF-β1-driven fibroblast differentiation (Fig. 3H, I). In addition, we validated our findings in A549 cells to enhance the robustness of our study (Additional file 2: Fig. S10).

We examined the therapeutic potential of *BRSK2* in a murine model of pulmonary fibrosis. Mice received aerosolized PBS, PEI/siCtrl, or PEI/si-*BRSK2* every 2 days for seven doses (Fig. 3J). While significant weight loss was noted post-bleomycin (BLE) administration in both PEI/siCtrl and PEI/si-*BRSK2* groups, the latter showed less weight reduction (Fig. 3K). On day 21, the lungs were harvested and analyzed. Ashcroft scores confirmed that BLE induced pulmonary fibrosis in mice, showing severe structural distortion and enlarged fibrotic areas, whereas inhalation of PEI/si-*BRSK2* mitigated these fibrotic levels (Fig. 3L). Histological analysis showed marked alveolar wall thickening, inflammatory cell infiltration, and increased collagen deposition in the PEI/siCtrl group. In contrast, PEI/si-*BRSK2* treatment significantly reduced α-SMA and *Col1A1* levels (Fig. 3M). The hydroxyproline assay indicated a significant decrease in

Table 2 SMR analysis results for *BRSK2* and IPF complication and prognosis

Exposure (<i>BRSK2</i>)	Outcome	TopSNP	OR	Lower OR Ci95	Upper OR Ci95	Pval	Nsnp	Pval (HEIDI)
GTEX-Lung	ILD-related respiratory insufficiency	rs7395567	1.437	0.998	2.070	5.131E-02	8	2.478E-03
GTEX-Lung	Transplant-free survival	rs4255564	0.782	0.518	1.179	2.409E-01	7	1.462E-01
UKBPPP-Blood	ILD-related respiratory insufficiency	rs7395567	1.191	1.006	1.411	4.200E-02	20	8.124E-11
UKBPPP-Blood	Transplant-free survival	rs7932863	0.859	0.709	1.042	1.233E-01	20	1.028E-02
deCODE-Blood	ILD-related respiratory insufficiency	rs4881748	3.879	2.058	7.311	2.754E-05	20	6.552E-05
deCODE-Blood	Transplant-free survival	rs4881748	0.481	0.240	0.964	3.909E-02	20	4.104E-02
eQTLGen-Blood	ILD-related respiratory insufficiency	rs11603658	5.802	1.118	30.105	3.634E-02	20	7.281E-02
eQTLGen-Blood	Transplant-free survival	rs11603658	0.249	0.047	1.317	1.018E-01	20	7.445E-02

ILD, interstitial lung disease; OR, odds ratios; CI, confidence interval; SMR, summary data-based Mendelian randomization; HEIDI, heterogeneity in the dependent instrument

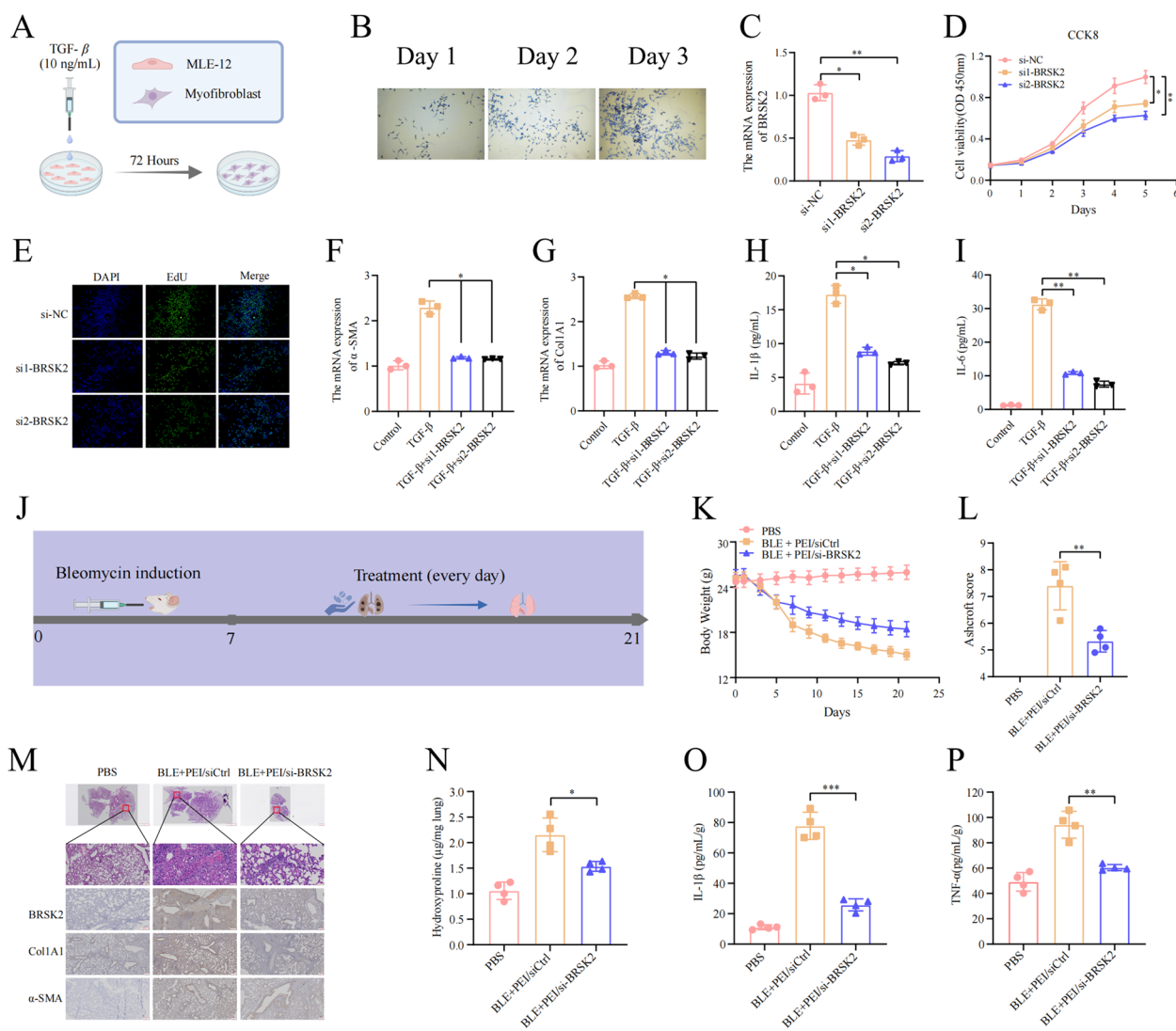


Fig. 3 *BRSK2* deficiency alleviates bleomycin-induced pulmonary fibrosis in vitro and in vivo. **A** Schematic diagram illustrating the experimental setup. **B** Masson’s trichrome staining of MLE-12 cells observed at various time points. **C** Validation of *BRSK2* mRNA expression by quantitative RT-PCR (qRT-PCR). **D, E** Assessment of cell viability using CCK-8 and EdU incorporation assays. **F, G** qRT-PCR analysis confirming mRNA expression levels of α -SMA and *Col1A1*. **H, I** Measurement of IL-1 β and IL-6 secretion via ELISA. **J** Schematic illustration depicting the design of the animal experiments. **K** Graph showing weight changes in mice across different experimental groups. **L** Ashcroft score analysis for evaluating fibrosis severity in mice from various groups. **M** Histological staining (HE, α -SMA, and *Col1A1*) demonstrating that treatment with *BRSK2* mitigates BLE-induced lung morphological alterations and fibrotic area expansion (scale bars: 2mm and 200 μ m). **(N)** Quantitative assessment of hydroxyproline (HYP) levels in mice following various treatments, conducted using HYP assays. **O** Measurement of IL-1 β concentrations in lung tissues of mice post-treatment. **P** Analysis of TNF- α concentrations in lung tissues of mice across different groups. Statistical significance between groups was determined using two-sided unpaired t-tests. * means *P*val < 0.05, and ** means *P*val < 0.01. Data are presented as mean \pm standard deviation (SD)

hydroxyproline levels in the PEI/si-*BRSK2* group, highlighting its therapeutic effects (Fig. 3N). ELISA results also showed elevated IL-1 β and TNF- α levels in pulmonary fibrosis mice, which were significantly reduced following PEI/si-*BRSK2* treatment, suggesting its efficacy in mitigating the cytokine storm associated with pulmonary fibrosis (Fig. 3O, P).

Association of BRSK2 downstream molecules with IPF

Based on previous findings, we investigated the mediating role of plasma protein components from the deCODE and UKBPPP studies in IPF risk using mRNA expression levels of *BRSK2* in lung tissues from GTEx and eQTLGen blood tissues. Mediator analyses of IVW and cML-MA identified 20 mediators (*BRSK2*, *COLEC12*, *CTRL*, *CTSD*, *CTSH*, *DLL4*, *GSTA3*, *GZMM*, *ICAM5*, *IFNAR1*, *IL1RN*,

LILRA5, *MIA*, *NTN1*, *PON3*, *PRSS2*, *PSMB1*, *TALDO1*, *TREM2*, *VEGFA*) that may act as downstream pathogenic molecules for *BRSK2* (Additional file 1: Tables S18–S19, Fig. 4A). Besides the *BRSK2* protein, the remaining mediators contributed to 0.537–22.106% of the mediation effect. Our colocalization analysis of the three protein sources and three endpoint sources indicated that 11 *BRSK2* downstream facilitators (*BRSK2*, *CTRL*, *CTSD*, *CTSH*, *DLL4*, *IL1RN*, *NTN1*, *PON3*, *PSMB1*, *TALDO1*, *VEGFA*) could be driven by the same causal variant in IPF development, with strong colocalization support

for *PSMB1* in the deCODE study and IPF data from the FinnGen study (PPH4=0.800, PPH3+4=0.890) (Additional file 1: Table S20, Fig. 4B–C). In GSE150910 ($n=103$ samples), *BRSK2* expression in lung tissues from IPF patients correlated with the expression levels of 12 *BRSK2* mediators, with strong association coefficients for *PSMB1*, *CTSD*, and *CTSH* (Additional file 1: Table S21, Fig. 4C). Additionally, in both animal and human-derived cellular models, we validated the expression changes of eight downstream molecules, including *PSMB1*, upon *BRSK2* silencing (Additional file 2: Fig. S11).

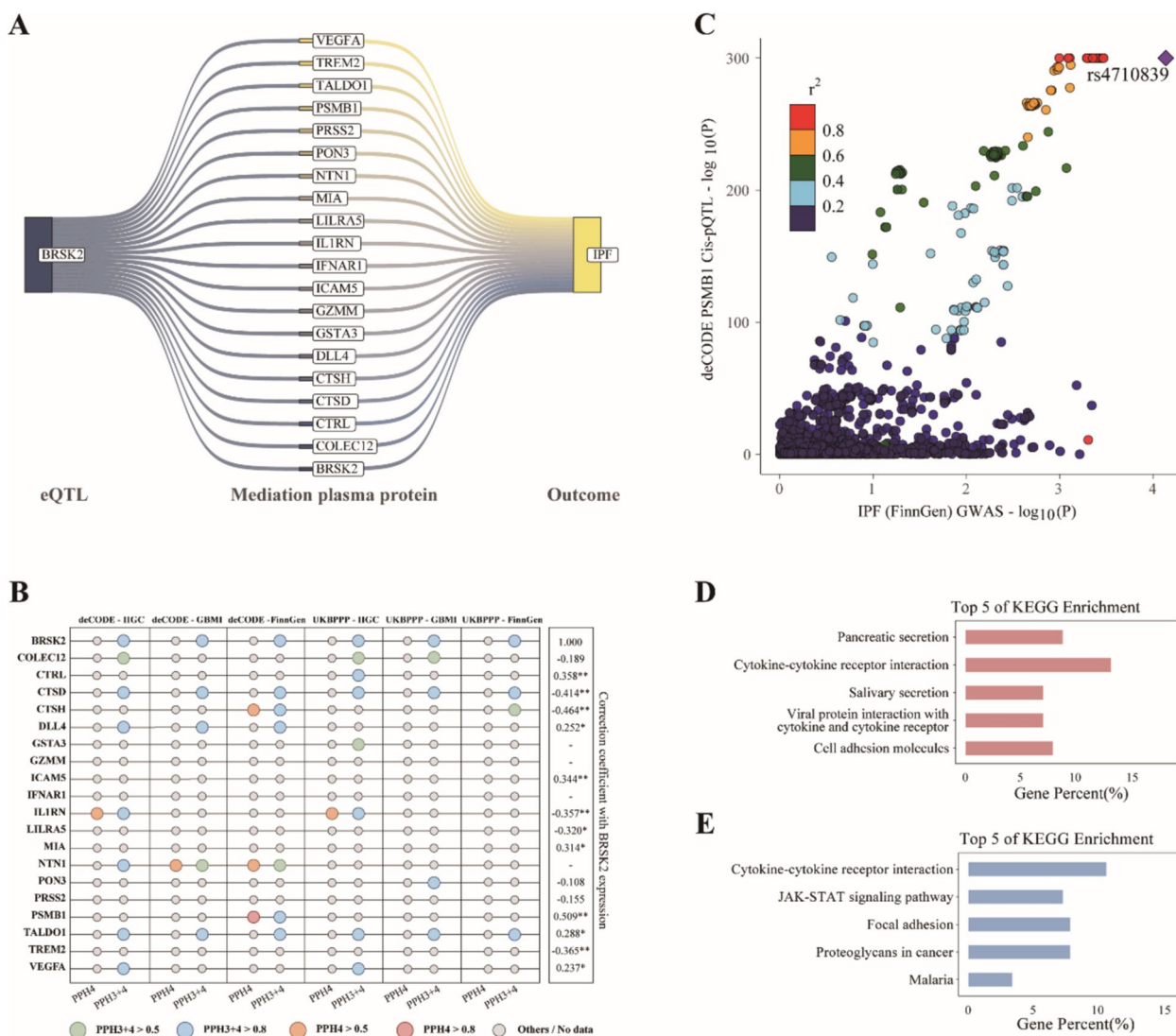


Fig. 4 Potential plasma protein mechanisms by which *BRSK2* promotes IPF. **A** Sankey diagram of plasma protein-mediated pathways for *BRSK2* to promote the development of IPF. **B** Colocalization analysis of Cis-pQTL for *PSMB1* (deCODE) and GWAS for IPF (FinnGen). **C** Colocalization analysis of *BRSK2* promoting IPF mediation protein and IPF. **D** KEGG enrichment analysis of blood *BRSK2* (eQTLGen) affecting plasma protein content. **E** KEGG enrichment analysis of lung *BRSK2* (GTEx) affecting plasma protein content. IPF, idiopathic pulmonary fibrosis; GWAS, genome-wide association study; eQTL, expression quantitative trait loci; pQTL, protein quantitative trait loci; PPH, posterior probabilities for hypotheses; KEGG, Kyoto Encyclopedia of Genes and Genomes

This confirmed that the plasma protein mechanism we identified is strongly correlated and consistent with the lung mechanism. Moreover, *PSMB1*, *CTSD*, and *CTSH* may serve as significant downstream molecules of *BRSK2* in promoting the progression of IPF. Further enrichment analyses suggested that *BRSK2* potentially impacts overall plasma protein levels, showing that changes in *BRSK2* in blood and lung tissue affecting plasma proteins were predominantly enriched in cytokine-cytokine receptor interactions (Fig. 4D, E).

Potential role of *BRSK2* Cis-mQTLs in IPF

To further explore how *BRSK2* might influence IPF, we investigated its regulation through DNA methylation. The analysis included 77 methylation probes and five outcomes, and after Bonferroni correction ($P_{val} < 1.299 \times 10^{-4}$) and HEIDI test, we identified seven specific loci in the *BRSK2* gene (cg03156651, cg07652408, cg11772193, cg14306344, cg16022876, cg16274762, and cg16793525) whose methylation levels were associated with IPF risk as well as *BRSK2* transcriptional or translational levels (Additional file 1: Table S22). From methylation to transcription to translation, a series of biological processes from epigenetic regulation to altered gene expression may be involved in the pathogenic effect of *BRSK2* on IPF.

PPI analysis and phenotype scan of IVs for *BRSK2*

A total of 31 drugs targeting 52 therapeutic pathways for IPF were identified (Additional file 1: Table S23). PPI analysis indicated that the therapeutic effects of clinically developed drugs, including Belumosudil, Taladegib, CC-90001, and ORIN1001, may involve the regulation of *BRSK2*. Additionally, *BRSK2* exhibited physical interactions with MAPT and co-expression relationships with MUC2 (Additional file 1: Table S24 and Additional file 2: Fig. S12).

To assess the extent to which *BRSK2*-related IVs were associated with IPF-related traits and confounders, we performed a phenotype scan of 11 related IVs. While no significant associations with IPF confounders were found, five SNPs (rs4881748, rs56321310, rs72849425, rs7932863, and rs10794293) were significantly linked to IPF-related traits (Additional file 2: Fig. S12), suggesting that the pathogenic effect of *BRSK2* in IPF may be driven by multiple causal sites.

Discussion

Identifying and validating disease progression targets through multi-omics approaches is essential for precision medicine. Recent studies underscore the importance

of multi-omics in discovering disease-specific therapeutic targets, which can aid in the development of targeted treatment strategies for disease progression [39–41]. This study initially screened 17 potential IPF treatment targets, with *BRSK2* emerging as the most promising due to its supportive evidence and shared causal variants with IPF at the tissue-specific level. *BRSK2* may also be linked to complications and reduced survival in IPF patients. The antifibrotic potential of *BRSK2* silencing was validated in both cellular and animal models, confirming its therapeutic value. The study also uncovered the potential pathogenic mechanism of *BRSK2* through plasma protein analysis and validated it in IPF tissues. *PSMB1*, *CTSD*, and *CTSH* were identified as key downstream targets in IPF development. Furthermore, altering *BRSK2* expression through epigenetic manipulation of methylation levels in the lung or plasma presents promising therapeutic prospects.

BRSK2 is a serine/threonine protein kinase located in the centrosome and endoplasmic reticulum, playing roles in cell apoptosis and cell polarity [42, 43], which are crucial for normal physiology and disease development. As part of the *AMPK* family, *BRSK2* influences cellular metabolism, cancer progression, and other biological processes. Research identifies *BRSK2* as a downstream mediator of *mTORC1* signaling and an indirect activator of the *AKT* pathway [44, 45]. Alterations in these pathways may contribute to IPF progression [46–48]. In IPF, *BRSK2* serves as a key pathogenic factor and is located adjacent to *TOLLIP*, a known susceptibility locus, which itself neighbors *MUC5B*, a well-established genetic determinant of IPF [49, 50]. This chromosomal proximity suggests potential interactions between *BRSK2*, *TOLLIP*, and *MUC5B* in the pathogenesis of IPF, warranting further investigation. Additionally, PheWAS analysis revealed a potential association between *BRSK2* and neurological phenotypes, such as gray matter changes in the temporal pole, aligning with prior studies linking deleterious *BRSK2* variants to neurodevelopmental disorders [51]. While *BRSK2* shows significant therapeutic potential in IPF, its possible neurological side effects require careful consideration in future research, particularly through the development of targeted strategies that avoid crossing the blood–brain barrier, to balance therapeutic efficacy and safety. Future research should focus on developing targeted therapies that modulate *BRSK2* expression, such as small molecule inhibitors or gene therapy. Additionally, investigating the interactions between *BRSK2* and key pathways like *mTORC1* and *AKT* may lead to the development of combination therapies that enhance efficacy while reducing side effects. Clinical trials to translate *BRSK2*-targeted therapies into practical applications for IPF are crucial to realizing its clinical potential.

Previous studies align with our findings, emphasizing key pathways in IPF pathogenesis. Reduced DEPTOR expression is associated with increased IPF susceptibility [3]. MR analyses have linked the regulation of MAPT and USP28 to IPF progression [52, 53], while the non-coding variant rs7934606 in MUC2 has been identified as an IPF risk locus in European populations [54]. POLR2L is considered a candidate gene for IPF-related genetic mechanisms [55], and the STN1-CTC1 complex may influence ILD via telomere regulation [56]. Protein interaction analyses revealed that *BRSK2* is associated with MAPT and MUC2 and interacts with multiple known IPF therapeutic targets. Among *BRSK2* downstream molecules, the *IFNAR1* family is involved in immune conditioning during pulmonary fibrosis [57], genetic polymorphisms in *IL1RN* play a role in IPF pathogenesis [58], macrophages drive pulmonary fibrosis progression via *NTN1* [59], and *TREM2* insufficiency attenuates fibrosis through macrophage polarization via *STAT6* activation [60]. *VEGFA*'s different expression patterns result in varied preventive or progressive outcomes in IPF [61]. Collectively, these findings identify *BRSK2* as a central node in IPF signaling, warranting further investigation into its regulatory mechanisms and therapeutic potential.

Pleiotropy has always been a crucial potential factor affecting MR analysis results [62]. Interestingly, a previous comment highlighted that positive outcomes of colocalization analysis might not necessarily strengthen the meaningful conclusions derived from the IVW method in MR studies. Instead, it is more likely to introduce pleiotropy, violating the exclusivity assumption of MR analysis [63]. Additionally, using the MR Egger intercept method to assess pleiotropy encounters issues of low efficiency and limited applicability. Therefore, it is important to extensively explore pleiotropy in MR research to ensure the robustness of the conclusions. Our study has employed various methods to reduce research bias caused by this factor. The cML-MA analysis method efficiently controls horizontal pleiotropy while managing Type I errors, and the cML-MA-BIC analysis results of this study also align with the IVW results. Furthermore, we conducted a phenotypic scan to explore the potential pleiotropy of *BRSK2*. The analysis found no evidence that the major IVs for *BRSK2* were associated with IPF confounders. It also revealed that multiple variants collectively influence IPF-related traits and *BRSK2* abundance. While this might subjectively suggest pleiotropy, when integrated with findings from other pleiotropy assessments, it more likely indicates additional colocalization sites between *BRSK2* expression levels and IPF occurrence. These results complement the colocalization analyses and HEIDI tests, further supporting the presence of

shared causal variants between *BRSK2* and IPF in this study. The strategy of predicting gene expression levels with SNPs in cis-regulatory sites minimizes the impact of horizontal pleiotropy caused by SNPs in non-regulatory regions. In summary, our analysis provides a multidimensional exploration of the pleiotropy issue in the main analysis results, thereby strengthening the credibility of our findings.

Several limitations warrant consideration in interpreting our findings. Firstly, our data predominantly originate from European population, which may not universally represent the genetic variations and environmental interactions inherent to other ethnicities. This highlights the need for replicating studies across diverse demographic groups to validate and generalize our conclusions. Secondly, a lack of overlap in QTLs data poses significant challenges, such as isolated positive eQTLs results without corroborative pQTLs findings could lead to spurious associations, thus affecting the reliability of gene-disease linkages identified in our study. Thirdly, discrepancies between QTLs across transcriptomic and proteomic datasets, as well as variability within the same omics layer across different studies, add complexity to the interpretation. Differences in gene expression profiles between plasma and tissues or organs, influenced by factors affecting transcription and translation, may contribute to inconsistencies, aligning with the substantial heterogeneity observed in our meta-analysis. Nevertheless, *BRSK2* demonstrated robust pathogenic effects in IPF under the random-effects model, further highlighting its significant therapeutic potential. Fourthly, despite efforts to control pleiotropy, the possibility of false positives remains. Fifthly, stringent variable screening and correction methods may inadvertently exclude viable therapeutic targets. Genes significant in multiple replication analyses before correction remain valuable for future research. Finally, we preliminarily explored the function of *BRSK2* and did not fully investigate its impact on inflammatory cell recruitment and function. In the future, more in-depth experiments, such as flow cytometry (FACS), immunohistochemistry (IHC), and immunofluorescence (IF), will be necessary to study these effects. Additionally, advanced nanocarrier delivery techniques should be utilized to enhance the efficiency, stability, and specificity of siRNA-*BRSK2* delivery to lung tissues, further improving therapeutic outcomes for targeting *BRSK2* in IPF.

Conclusions

Comprehensive MR analyses highlighted the potential of the genetic agent *BRSK2* for treating IPF and improving prognosis, with preliminary safety assessed via PheWAS. In vivo experiments confirmed *BRSK2*'s therapeutic efficacy as an anti-fibrotic agent. Further mechanistic

studies indicated that *PSMB1*, *CTSD*, and *CTSH* may contribute to *BRSK2*'s effects on pulmonary fibrosis, with DNA methylation playing a crucial role in its pathogenic mechanism. These findings suggest additional experimental designs for future research and offer new directions for developing therapies for pulmonary fibrosis.

Abbreviations

IPF	Idiopathic pulmonary fibrosis
QTLs	Quantitative trait loci
GWAS	Genome-Wide Association Studies
MR	Mendelian randomization
eQTL	Expression quantitative trait loci
pQTL	Protein quantitative trait loci
mQTL	Methylation quantitative trait loci
HEIDI	Heterogeneity in the dependent instrument
PheWAS	Phenome-wide association study
PRFs	Potential risk factors
IVs	Instrumental variables
MAF	Minor allele frequency
IVW	Inverse variance weighted
LDSC	Linkage disequilibrium score regression
GOF	Goodness-of-fit
PP	Posterior probabilities
SMR	Summary data-based Mendelian randomization analysis
ILD	Interstitial lung disease
GBMI	Global Biobank Meta-analysis Initiative
IIGC	International IPF Genetics Consortium
DLCO	Diffusing capacity of the lung for carbon monoxide
FVC	Forced vital capacity

Supplementary Information

The online version contains supplementary material available at <https://doi.org/10.1186/s12916-025-03848-y>.

Supplementary Material 1.

Supplementary Material 2: Figure S1. Screening MR flowchart for IPF drug target. IPF: idiopathic pulmonary fibrosis; eQTL: expression quantitative trait loci; pQTL: protein quantitative trait loci; IIGC: International IPF Genetics Consortium; GBMI: Global Biobank Meta-analysis Initiative. Figure S2. Heatmaps of 17 potential IPF targets in 15 MR analysis combinations by IVW or Wald ratio methods. MR: mendelian randomization; IPF: idiopathic pulmonary fibrosis; IVW: inverse variance weighted; IIGC: International IPF Genetics Consortium; GBMI: Global Biobank Meta-analysis Initiative. * means $P_{val} < 0.05$, and ** means $P_{val} < 0.05$ after Bonferroni correction. Figure S3. Heatmaps of 17 potential IPF targets in 15 MR analysis combinations by cML-MA methods. MR: mendelian randomization; IPF: idiopathic pulmonary fibrosis; cML-MA: constrained maximum likelihood and model averaging; IIGC: International IPF Genetics Consortium; GBMI: Global Biobank Meta-analysis Initiative. * means $P_{val} < 0.05$, and ** means $P_{val} < 0.05$ after Bonferroni correction. Figure S4. Heatmaps of 17 potential IPF targets in 15 MR analysis combinations by SMR methods. MR: mendelian randomization; IPF: idiopathic pulmonary fibrosis; SMR: summary data-based mendelian randomization; IIGC: International IPF Genetics Consortium; GBMI: Global Biobank Meta-analysis Initiative. * means $P_{val} < 0.05$, and ** means $P_{val} < 0.05$ after Bonferroni correction. Figure S5. Forest plot of the meta-analysis results of the TSMR analysis between *BRSK2* and IPF at the transcriptomic level. (A) Meta-analysis of IVW/Wald ratio results. (B) Meta-analysis of IVW/Wald ratio results. TSMR: two sample mendelian randomization; IPF: idiopathic pulmonary fibrosis; SMR: summary data-based mendelian randomization; IIGC: International IPF Genetics Consortium; GBMI: Global Biobank Meta-analysis Initiative; OR: odds ratios; CI: confidence interval. Figure S6. Forest plot of the meta-analysis results of the TSMR analysis between *BRSK2* and IPF at the translation-level. (A) Meta-analysis of IVW/Wald ratio results. (B) Meta-analysis of IVW/Wald ratio results. TSMR: two sample mendelian randomization; IPF: idiopathic pulmonary fibrosis; SMR: summary data-based mendelian randomization;

IIGC: International IPF Genetics Consortium; GBMI: Global Biobank Meta-analysis Initiative; OR: odds ratios; CI: confidence interval. Figure S7. Schematic diagram of the principle of two-step mediation analysis. TSMR: two sample mendelian randomization; IPF: idiopathic pulmonary fibrosis. Figure S8. PheWAS manhattan plots of *BRSK2* with binary and continuous traits. In the figure, different colors represent different types of phenotypes, with each point or triangle representing a specific phenotype. Upward-facing triangles indicate that an increase in gene expression level is associated with an increased risk of the corresponding phenotype. When a point lies above the dashed line corresponding to the suggested threshold, it indicates that the PheWAS result exceeds the recommended significance level. PheWAS: phenome-wide association study. Figure S9. Expression of *BRSK2* in IPF patients and association with respiratory function indices. (A) Comparison of *BRSK2* expression in IPF lung tissue and normal tissue. (B) *BRSK2* expression comparison in PBMCs between IPF patients and healthy controls. (C) Correlation between *BRSK2* expression in PBMCs and DLCO in IPF patients. (D) Correlation between *BRSK2* expression in PBMCs and FVC%pred in IPF patients. DLCO: Diffusing capacity of the lung for carbon monoxide; FVC: Forced vital capacity. Figure S10. Knockdown *BRSK2* alleviates fibrosis in A549 cells. (A) Assessment of cell viability using CCK-8 assays. (B) Validation of *BRSK2* mRNA expression by quantitative RT-PCR (qRT-PCR). (C-D) qRT-PCR analysis confirming mRNA expression levels of α -SMA and *Col1A1*. (E-F) Measurement of IL-1 β and IL-6 secretion via ELISA. Statistical significance between groups was determined using two-sided unpaired t-tests. * means $P_{val} < 0.05$, and ** means $P_{val} < 0.01$. Figure S11. Verify the downstream molecules of *BRSK2*. (A) qRT-PCR analysis confirming mRNA expression levels of downstream molecules in A549 cells. (B) qRT-PCR analysis confirming mRNA expression levels of downstream molecules in animal model. Statistical significance between groups was determined using two-sided unpaired t-tests. n.s means no significance, * means $P_{val} < 0.05$, and ** means $P_{val} < 0.01$. Figure S12. PPI analysis and phenotypic scanning network for *BRSK2*.

Supplementary Material 3.

Supplementary Material 4.

Acknowledgements

We gratefully acknowledge the invaluable contributions from researchers at prestigious institutions including the UK Biobank, the deCODE project, the Fenland study, the GTEX project, the McRae study and the eQTLGen consortium, who have significantly advanced quantitative trait loci research. Our sincere appreciation is also extended to the participants of the International IPF Genetics Consortium, the Global Biobank Meta-analysis study, and the Finngen study, who have actively participated and generously shared their genome-wide association studies data on idiopathic pulmonary fibrosis. Furthermore, we express our gratitude towards the diligent researchers and dedicated participants of other genome-wide association studies datasets used in this study. Their steadfast commitment has been crucial in propelling scientific advancements. We also thank BioRender.com for their assistance with illustrations.

Authors' contributions

The study was conceptualized by ZC and KX. The design was developed by ZC, KX, JL2, and HM. Data curation and analysis were performed by ZC, MT, NW, and JL1. The MR analysis was supervised by KX, JL2, and HM. Data interpretation was carried out by ZC, MT, and XT. All authors read and approved the final manuscript.

Funding

This study was supported by the National Natural Science Foundation of China (No. 82273325), Medical and industrial collaborative innovation research project (No. SZM2021005) and Medical Innovation Application Research in the Science and Technology Special Project (No. SZM2023029).

Data availability

No datasets were generated or analysed during the current study.

Declarations

Ethics approval and consent to participate

The study was approved by the Institutional Animal Care and Use Committee at Soochow University Medical Center (the Fourth Affiliated Hospital of Soochow University, Suzhou Dushu Lake Hospital) Laboratory Animal Center (Application ID:241136).

Consent for publication

Not applicable.

Competing interests

The authors declare no competing interests.

Author details

¹Department of Cardiothoracic Surgery, The Fourth Affiliated Hospital of Soochow University, Suzhou 215000, China. ²Department of Infectious Diseases, The First Affiliated Hospital of Anhui Medical University, Hefei 230022, China. ³Department of Cardiothoracic Surgery, Jinling Hospital, Medical School of Nanjing University, Nanjing, China.

Received: 7 August 2024 Accepted: 7 January 2025

Published online: 21 January 2025

References

- Maher TM, Bendstrup E, Dron L, Langley J, Smith G, Khalid JM, et al. Global incidence and prevalence of idiopathic pulmonary fibrosis. *Respir Res*. 2021;22(1):197.
- Bonella F, Spagnolo P, Ryerson C. Current and Future Treatment Landscape for Idiopathic Pulmonary Fibrosis. *Drugs*. 2023;83(17):1581–93.
- Allen RJ, Guillen-Guio B, Oldham JM, Ma SF, Drossen A, Paynton ML, et al. Genome-Wide Association Study of Susceptibility to Idiopathic Pulmonary Fibrosis. *Am J Respir Crit Care Med*. 2020;201(5):564–74.
- Wu X, Li W, Luo Z, Chen Y. The minor T allele of the MUC5B promoter rs35705950 associated with susceptibility to idiopathic pulmonary fibrosis: a meta-analysis. *Sci Rep*. 2021;11(1):24007.
- Little M. Mendelian Randomization: Methods for using Genetic Variants in Causal Estimation. *J R Stat Soc Ser A Stat Soc*. 2018;181(2):549–50.
- The Genotype-Tissue Expression (GTEx) project. *Nat Genet*. 2013;45(6):580–5.
- Vösa U, Claringbould A, Westra HJ, Bonder MJ, Deelen P, Zeng B, et al. Large-scale cis- and trans-eQTL analyses identify thousands of genetic loci and polygenic scores that regulate blood gene expression. *Nat Genet*. 2021;53(9):1300–10.
- Ferkingstad E, Sulem P, Atlason BA, Sveinbjornsson G, Magnusson MI, Styrudottir EL, et al. Large-scale integration of the plasma proteome with genetics and disease. *Nat Genet*. 2021;53(12):1712–21.
- Sun BB, Chiou J, Traylor M, Benner C, Hsu YH, Richardson TG, et al. Plasma proteomic associations with genetics and health in the UK Biobank. *Nature*. 2023;622(7982):329–38.
- Allen RJ, Stockwell A, Oldham JM, Guillen-Guio B, Schwartz DA, Maher TM, et al. Genome-wide association study across five cohorts identifies five novel loci associated with idiopathic pulmonary fibrosis. *Thorax*. 2022;77(8):829–33.
- Oldham JM, Allen RJ, Lorenzo-Salazar JM, Molyneaux PL, Ma SF, Joseph C, et al. PCSK6 and Survival in Idiopathic Pulmonary Fibrosis. *Am J Respir Crit Care Med*. 2023;207(11):1515–24.
- Kurki MI, Karjalainen J, Palta P, Sipilä TP, Kristiansson K, Donner KM, et al. FinnGen provides genetic insights from a well-phenotyped isolated population. *Nature*. 2023;613(7944):508–18.
- Zhou W, Kanai M, Wu KH, Rasheed H, Tsuo K, Hirbo JB, et al. Global Biobank Meta-analysis Initiative: Powering genetic discovery across human disease. *Cell Genom*. 2022;2(10):100192.
- Liu M, Jiang Y, Wedow R, Li Y, Brazel DM, Chen F, et al. Association studies of up to 1.2 million individuals yield new insights into the genetic etiology of tobacco and alcohol use. *Nat Genet*. 2019;51(2):237–44.
- Yengo L, Sidorenko J, Kemper KE, Zheng Z, Wood AR, Weedon MN, et al. Meta-analysis of genome-wide association studies for height and body mass index in ~700000 individuals of European ancestry. *Hum Mol Genet*. 2018;27(20):3641–9.
- Ong JS, An J, Han X, Law MH, Nandakumar P, Schumacher J, et al. Multitrait genetic association analysis identifies 50 new risk loci for gastro-oesophageal reflux, seven new loci for Barrett's oesophagus and provides insights into clinical heterogeneity in reflux diagnosis. *Gut*. 2022;71(6):1053–61.
- Lin J, Zhou J, Xu Y. Potential drug targets for multiple sclerosis identified through Mendelian randomization analysis. *Brain*. 2023;146(8):3364–72.
- Papadimitriou N, Dimou N, Tsilidis KK, Banbury B, Martin RM, Lewis SJ, et al. Physical activity and risks of breast and colorectal cancer: a Mendelian randomisation analysis. *Nat Commun*. 2020;11(1):597.
- Xue H, Shen X, Pan W. Constrained maximum likelihood-based Mendelian randomization robust to both correlated and uncorrelated pleiotropic effects. *Am J Hum Genet*. 2021;108(7):1251–69.
- Zhu Z, Zhang F, Hu H, Bakshi A, Robinson MR, Powell JE, et al. Integration of summary data from GWAS and eQTL studies predicts complex trait gene targets. *Nat Genet*. 2016;48(5):481–7.
- McRae AF, Marioni RE, Shah S, Yang J, Powell JE, Harris SE, et al. Identification of 55,000 Replicated DNA Methylation QTL. *Sci Rep*. 2018;8(1):17605.
- Wu Y, Zeng J, Zhang F, Zhu Z, Qi T, Zheng Z, et al. Integrative analysis of omics summary data reveals putative mechanisms underlying complex traits. *Nat Commun*. 2018;9(1):918.
- Chen J, Ruan X, Sun Y, Lu S, Hu S, Yuan S, et al. Multi-omic insight into the molecular networks of mitochondrial dysfunction in the pathogenesis of inflammatory bowel disease. *EBioMedicine*. 2024;99:104934.
- Skrivankova VW, Richmond RC, Woolf BAR, Davies NM, Swanson SA, VanderWeele TJ, et al. Strengthening the reporting of observational studies in epidemiology using mendelian randomisation (STROBE-MR): explanation and elaboration. *BMJ*. 2021;375:n2233.
- Wang Q, Dhindsa RS, Carss K, Harper AR, Nag A, Tachmazidou I, et al. Rare variant contribution to human disease in 281,104 UK Biobank exomes. *Nature*. 2021;597(7877):527–32.
- Yuan S, Xu F, Li X, Chen J, Zheng J, Mantzoros CS, et al. Plasma proteins and onset of type 2 diabetes and diabetic complications: Proteome-wide Mendelian randomization and colocalization analyses. *Cell Rep Med*. 2023;4(9):101174.
- Su WM, Gu XJ, Dou M, Duan QQ, Jiang Z, Yin KF, et al. Systematic drug-gable genome-wide Mendelian randomisation identifies therapeutic targets for Alzheimer's disease. *J Neurol Neurosurg Psychiatry*. 2023;94(11):954–61.
- Jaffar J, Wong M, Fishbein GA, Alhamdoosh M, McMillan L, Gamell-Fulla C, et al. Matrix metalloproteinase-7 is increased in lung bases but not apices in idiopathic pulmonary fibrosis. *GEO <https://www.ncbi.nlm.nih.gov/geo/query/acc.cgi?acc=GSE213001>*. 2022.
- Huang LS, Berdyshev EV, Tran JT, Xie L, Chen J, Ebenezer DL, et al. Sphingosine-1-phosphate lyase is an endogenous suppressor of pulmonary fibrosis: role of S1P signalling and autophagy. *GEO <https://www.ncbi.nlm.nih.gov/geo/query/acc.cgi?acc=GSE38958>*. 2014.
- Furusawa H, Cardwell JH, Okamoto T, Walts AD, Konigsberg IR, Kurche JS, et al. Chronic Hypersensitivity Pneumonitis, an Interstitial Lung Disease with Distinct Molecular Signatures. *GEO <https://www.ncbi.nlm.nih.gov/geo/query/acc.cgi?acc=GSE150910>*. 2020.
- Campa CC, Silva RL, Margaria JP, Pirali T, Mattos MS, Kraemer LR, et al. Inhalation of the prodrug PI3K inhibitor CL27c improves lung function in asthma and fibrosis. *Nat Commun*. 2018;9(1):5232.
- Werth S, Urban-Klein B, Dai L, Höbel S, Grzelinski M, Bakowsky U, et al. A low molecular weight fraction of polyethylenimine (PEI) displays increased transfection efficiency of DNA and siRNA in fresh or lyophilized complexes. *J Control Release*. 2006;112(2):257–70.
- Höbel S, Aigner A. Polyethylenimine (PEI)/siRNA-mediated gene knock-down in vitro and in vivo. *Methods Mol Biol*. 2010;623:283–97.
- Kilkenny C, Browne WJ, Cuthill IC, Emerson M, Altman DG. Improving bioscience research reporting: the ARRIVE guidelines for reporting animal research. *PLoS Biol*. 2010;8(6):e1000412.
- Yuan S, Xu F, Zhang H, Chen J, Ruan X, Li Y, et al. Proteomic insights into modifiable risk of venous thromboembolism and cardiovascular comorbidities. *J Thromb Haemost*. 2024;22(3):738–48.
- Zhu J, Zhou D, Yu M, Li Y. Appraising the causal role of smoking in idiopathic pulmonary fibrosis: a Mendelian randomization study. *Thorax*. 2024;79(2):179–81.

37. Zhu J, Zhou D, Wang J, Yang Y, Chen D, He F, et al. A Causal Atlas on Comorbidities in Idiopathic Pulmonary Fibrosis: A Bidirectional Mendelian Randomization Study. *Chest*. 2023;164(2):429–40.
38. Wu W, Li C, Zhu X, Liu X, Li P, Wan R, et al. Genetic association of telomere length, obesity and tobacco smoking with idiopathic pulmonary fibrosis risk. *BMC Public Health*. 2023;23(1):868.
39. Wang Y, Ji B, Zhang L, Wang J, He J, Ding B, et al. Identification of metastasis-related genes for predicting prostate cancer diagnosis, metastasis and immunotherapy drug candidates using machine learning approaches. *Biol Direct*. 2024;19(1):50.
40. Wang Y, He J, Zhao Q, Bo J, Zhou Y, Sun H, et al. Evaluating the predictive value of angiogenesis-related genes for prognosis and immunotherapy response in prostate adenocarcinoma using machine learning and experimental approaches. *Front Immunol*. 2024;15:1416914.
41. Wang Y, Li C, He J, Zhao Q, Zhou Y, Sun H, et al. Multi-omics analysis and experimental validation of the value of monocyte-associated features in prostate cancer prognosis and immunotherapy. *Front Immunol*. 2024;15:1426474.
42. Wang Y, Wan B, Li D, Zhou J, Li R, Bai M, et al. BRSK2 is regulated by ER stress in protein level and involved in ER stress-induced apoptosis. *Biochem Biophys Res Commun*. 2012;423(4):813–8.
43. Kishi M, Pan YA, Crump JG, Sanes JR. Mammalian SAD kinases are required for neuronal polarization. *Science*. 2005;307(5711):929–32.
44. Nie J, Liu X, Lilley BN, Zhang H, Pan YA, Kimball SR, et al. SAD-A kinase controls islet β -cell size and function as a mediator of mTORC1 signaling. *Proc Natl Acad Sci U S A*. 2013;110(34):13857–62.
45. Saiyin H, Na N, Han X, Fang Y, Wu Y, Lou W, et al. BRSK2 induced by nutrient deprivation promotes Akt activity in pancreatic cancer via downregulation of mTOR activity. *Oncotarget*. 2017;8(27):44669–81.
46. Rangarajan S, Bone NB, Zmijewska AA, Jiang S, Park DW, Bernard K, et al. Metformin reverses established lung fibrosis in a bleomycin model. *Nat Med*. 2018;24(8):1121–7.
47. Wang J, Hu K, Cai X, Yang B, He Q, Wang J, et al. Targeting PI3K/AKT signaling for treatment of idiopathic pulmonary fibrosis. *Acta Pharm Sin B*. 2022;12(1):18–32.
48. Yanagihara T, Tsubouchi K, Zhou Q, Chong M, Otsubo K, Isshiki T, et al. Vascular-Parenchymal Cross-Talk Promotes Lung Fibrosis through BMPR2 Signaling. *Am J Respir Crit Care Med*. 2023;207(11):1498–514.
49. Lorenzo-Salazar JM, Ma SF, Jou J, Hou PC, Guillen-Guio B, Allen RJ, et al. Novel idiopathic pulmonary fibrosis susceptibility variants revealed by deep sequencing. *ERJ Open Res*. 2019;5(2).
50. Noth I, Zhang Y, Ma SF, Flores C, Barber M, Huang Y, et al. Genetic variants associated with idiopathic pulmonary fibrosis susceptibility and mortality: a genome-wide association study. *Lancet Respir Med*. 2013;1(4):309–17.
51. Hiatt SM, Thompson ML, Prokop JW, Lawlor JMJ, Gray DE, Bebin EM, et al. Deleterious Variation in BRSK2 Associates with a Neurodevelopmental Disorder. *Am J Hum Genet*. 2019;104(4):701–8.
52. Zhang K, Shi P, Li A, Zhou J, Chen M. Plasma genome-wide mendelian randomization identifies potentially causal genes in idiopathic pulmonary fibrosis. *Respir Res*. 2024;25(1):379.
53. Zhu J, Liu H, Gao R, Gong R, Wang J, Zhou D, et al. Genetic-informed proteome-wide scan reveals potential causal plasma proteins for idiopathic pulmonary fibrosis. *Thorax*. 2024;79(9):878–82.
54. Kishore A, Žižková V, Kocourková L, Petrková J, Bouros E, Nunes H, et al. Association Study for 26 Candidate Loci in Idiopathic Pulmonary Fibrosis Patients from Four European Populations. *Front Immunol*. 2016;7:274.
55. Gong W, Guo P, Liu L, Guan Q, Yuan Z. Integrative Analysis of Transcriptome-Wide Association Study and mRNA Expression Profiles Identifies Candidate Genes Associated With Idiopathic Pulmonary Fibrosis. *Front Genet*. 2020;11:604324.
56. Liu L, Luo H, Sheng Y, Kang X, Peng H, Luo H, et al. A novel mutation of CTC1 leads to telomere shortening in a chinese family with interstitial lung disease. *Hereditas*. 2023;160(1):37.
57. Savigny F, Schricke C, Lacerda-Queiroz N, Meda M, Nascimento M, Huot-Marchand S, et al. Protective Role of the Nucleic Acid Sensor STING in Pulmonary Fibrosis. *Front Immunol*. 2020;11:588799.
58. Barlo NP, van Moorsel CH, Korthagen NM, Heron M, Rijkers GT, Ruven HJ, et al. Genetic variability in the IL1RN gene and the balance between interleukin (IL)-1 receptor agonist and IL-1 β in idiopathic pulmonary fibrosis. *Clin Exp Immunol*. 2011;166(3):346–51.
59. Gao R, Peng X, Perry C, Sun H, Ntokou A, Ryu C, et al. Macrophage-derived netrin-1 drives adrenergic nerve-associated lung fibrosis. *J Clin Invest*. 2021;131(1):e136542.
60. Luo Q, Deng D, Li Y, Shi H, Zhao J, Qian Q, et al. TREM2 Insufficiency Protects against Pulmonary Fibrosis by Inhibiting M2 Macrophage Polarization. *Int Immunopharmacol*. 2023;118:110070.
61. Barratt SL, Blythe T, Jarrett C, Ourradi K, Shelley-Fraser G, Day MJ, et al. Differential Expression of VEGF-A(xxx) Isoforms Is Critical for Development of Pulmonary Fibrosis. *Am J Respir Crit Care Med*. 2017;196(4):479–93.
62. Hemani G, Bowden J, Davey SG. Evaluating the potential role of pleiotropy in Mendelian randomization studies. *Hum Mol Genet*. 2018;27(R2):R195–r208.
63. Yin Q, Zhu L. Does co-localization analysis reinforce the results of Mendelian randomization? *Brain*. 2024;147(1):e7–8.

Publisher's Note

Springer Nature remains neutral with regard to jurisdictional claims in published maps and institutional affiliations.